ISSN 0965-5425, Computational Mathematics and Mathematical Physics, 2018, Vol. 58, No. 5, pp. 775–789. © Pleiades Publishing, Ltd., 2018.
Original Russian Text © I.A. Bedarev, A.V. Fedorov, A.V. Shul'gin, 2018, published in Zhurnal Vychislitel'noi Matematiki i Matematicheskoi Fiziki, 2018, Vol. 58, No. 5, pp. 806–820.

Computation of Traveling Waves in a Heterogeneous Medium with Two Pressures and a Gas Equation of State Depending on Phase Concentrations

I. A. Bedarev[a],*, A. V. Fedorov[a],, and A. V. Shul'gin[a],*****

[a] *Khristianovich Institute of Theoretical and Applied Mechanics, Siberian Branch, Russian Academy of Sciences, Novosibirsk, 630090 Russia*

**e-mail: bedarev@itam.nsc.ru*

***e-mail: fedorov@itam.nsc.ru*

****e-mail: shulgin@itam.nsc.ru*

Received March 29, 2017

Abstract—A fine structure theory of shock waves occurring in a gas–particle mixture was developed using an Anderson-type model with allowance for different phase pressures and with an equation of state for the gas component depending on the mean densities of both phases. The conditions for the formation of various types of shock waves based on the different speeds of sound in the phases were indicated. A high-order accurate TVD scheme was developed to prove the stability of some types of shock waves. The scheme was used to implement steadily propagating shock waves found in the stationary approximation, namely, shock waves of dispersive, frozen, and dispersive-frozen structures with one or two fronts.

Keywords: heterogeneous media with high particle concentrations, shock wave structure, numerical methods.

DOI: 10.1134/S0965542518050044

INTRODUCTION

The physical and mathematical description of waves propagating in mixtures of a gas and fine solid particles or liquid drops is a problem of interest in science and engineering. Indeed, numerous technological processes in various industries can be described by laws of the mechanics of heterogeneous media (MHM). Examples are the flow of gas mixture components through a loose catalyst with/without allowance for chemical reactions and the flow of concentrated suspensions in various ducts. Another example is the simulation of gas suspension formation caused by fine solid particles lifted from unstable sediment by blast and detonation waves [1–3]. The wind interaction with a fluid surface is also a problem of this class. Thus, there are numerous examples confirming the practical importance of the study of heterogeneous media flows at high concentrations of the discrete phase. To determine types of mixture flows, mutually penetrating motions of the phases and components have to be taken into account. Concerning dynamical phenomena in heterogeneous media, a problem of great interest is the interaction of porous layers, for example, a cell-porous structure and layers of particles with strong discontinuities in the bulk density (shock waves). Therefore, the determination of possible configurations of shock waves (frozen, dispersive, one-, and two-front configurations) is of great interest in this area of MHM. Solving this problem, we can understand which forms of strong discontinuities can occur in heterogeneous media and under which conditions they exist.

1. FORMULATION OF THE PROBLEM

1.1. Preliminary Remarks and an Overview of Works

Before formulating the problem, we briefly overview our works performed in this area of MHM. In [4] the shock structure problem in a mixture of a gas and solid particles with a common phase pressure was investigated with volume particle concentrations taken into account in the mathematical model, including the equation of state of the medium. The case of micro- and nanoparticles moving in an ideal or viscous

gas was considered. A rather comprehensive bibliography concerning this subject (up to the year 1986) can also be found in [4]. More specifically, it was shown in [4] that, if the initial velocity of the mixture is higher than the frozen speed of sound, then a frozen shock wave propagates in this medium. If the shock velocity belongs to the dispersion interval, then the shock wave represents a continuous compression wave, which is known as a dispersive shock wave. Note that the types of shock waves in a heterogeneous medium are close to those in nonequilibrium single-speed gases or other media. Undoubtedly, worth noting are the works of Nigmatulin's school [5] and V.M. Fomin's school in the given area. Additionally, shock wave structures in a mixture of a viscous gas and ultradispersive solid particles were considered in [4]. In a standard fashion, the study was reduced to qualitative analysis of a boundary value problem for a system of ordinary differential equations describing the formulated physical problem. The resulting assertions were illustrated by numerical computations.

The structure of combined discontinuities and shock waves was again addressed in [6–9]. These studies were based on the Anderson model (system of composite-type equations) and the Baer–Nunziato model (hyperbolic model).

Used in [4], Kh.A. Rakhmatulin's model is known to be valid when the volume concentrations of the solid phase are infinitesimal. As the amount of particles in the mixture grows, the particle pressure has to be taken into account, i.e., the model is transformed into one for granular media or heterogeneous media with allowance for chaotic pressure [7–9]. In [6] a model of this type was used to investigate the structure of a combined discontinuity, i.e., a strong discontinuity propagating in a mixture and having a jump only in the particle volume concentration. Such variants of discontinuities arise in the interaction of shock and detonation waves with the leading edge of a particle cloud [3]. In [6, 9] conditions on a combined discontinuity were derived, the flow in a finite cloud of particles was numerically determined, and similar flows in problems of a shock wave interacting with clouds of particles were indicated.

It is well known that the system of MHM equations has a composite type (some of the characteristics are real, and the others, imaginary) and is not conservative, except for rare simplified versions. The solvability of initial–boundary value problems for certain types of the indicated mathematical models with and without allowance for the particle pressure has been analyzed in recent years. In this case, difficulties are caused by the presence of a nonconservative term involving the product of the gas pressure and the gradient of the volume particle concentration. Without analyzing these approaches, we mention [10] as an example in which a new definition of the weak solution to a boundary value problem is given and numerical algorithms for its reproduction are constructed.

Thus, the construction of stationary/nonstationary exact solutions for these models and numerical schemes for their implementation presents doubtless interest. In this paper we use of the simplified version of mathematical model of a mixture used in [6–9], namely adiabatic version of the Anderson model [6, 11] for description of nonlinear motions of a granular medium.

Preliminarily, we mention [12, 13], where the shock structure problem in a gas mixture was considered in the special case where the gas pressure depends only on the mean gas density (with the volume particle concentration being neglected) and the nonconservative term is omitted from the equation of motion of the particles. In this case, the basic system of equations is hyperbolic [12]. The shock structure can be analyzed using the approach of [14, 15], where a similar problem (concerning the existence of a traveling-wave solution and its stability) was studied for the Baer–Nunziato model. The nonconservative term was taken into account in [13]. Additionally, a numerical scheme for solving initial–boundary value problems in the mechanics of heterogeneous media with two phase pressures was constructed in [13] and the stability of the resulting stationary solutions was shown. Note that, in contrast to gas–particle mixtures with a single common pressure, shock waves in the above-described flow with two phase pressures can have dispersive-frozen and two-front structures depending on the particle concentration ahead of the wavefront and the shock wave velocity.

In this paper, we do not assume that the equation of state of the gas is independent of the mean particle density, which physically corresponds to allowance for the volume particle concentration. Thus, we consider a more general case of flow as compared with the one described above.

1.2. Physical and Mathematical Formulation of the Problem

Consider a mixture of a gas and solid particles occupying a one-dimensional continuum. The motion of the mixture is described by a mathematical model of interpenetrating motion of two interacting continua with parameters of each (such as the velocity, density, and pressure) averaged over the volume. The first continuum is the continuous component of the mixture, i.e., the gas characterized by its velocity, pressure, and volume concentration. The second continuum consists of the particles.

The second continuum (particle phase) is physically discrete and is characterized by its pressure (which arises as the momentum transferred by the particles in their chaotic motion in the gas), its velocity, and its volume concentration, which are other than the gas parameters. With the pressure of the particle phase taken into account, the motion of the considered two-phase medium in the isothermal case is described by the mass and momentum conservation laws written for each phase and supplemented by equations of state (Anderson model) [11]:

$$\begin{gathered}\frac{\partial \rho_i}{\partial t}+\frac{\partial(\rho_i u_i)}{\partial x}=0,\\ \frac{\partial(\rho_1 u_1)}{\partial t}+\frac{\partial\left(\rho_1 u_1^2+m_1 p_1\right)}{\partial x}=p_1\frac{\partial m_1}{\partial x}+f_1,\\ \frac{\partial(\rho_2 u_2)}{\partial t}+\frac{\partial\left(\rho_2 u_2^2+m_2 p_1\right)}{\partial x}+\frac{\partial p_2}{\partial x}=p_1\frac{\partial m_2}{\partial x}+f_2,\\ p_1=p_1(\rho_1,\rho_2),\quad p_2=p_2(\rho_2),\quad i=1,2.\end{gathered}\tag{1}$$

In the isothermal case under consideration, we use equations of state in linear form for both phases:

$$p_1=\frac{a_1^2\rho_1}{1-m_2},\quad p_2=a_2^2\rho_2.\tag{2}$$

Here, $\rho_i=\rho_{ii}m_i$, ρ_{ii}, m_i, u_i, p_i, and a_i are the mean and true densities, volume concentration, velocity, pressure, and speed of sound of the ith phase ($i=1, 2$). The indices 1 and 2 denote the gas and particle parameters, respectively; f_1 is the force exerted by the gas on the particles; $f_2=-f_1$ is the force exerted by the particles on the gas; and the true particle density $\rho_{22}=r$ is a constant. System (1), (2) is closed by the basic MHM equality

$$m_1+m_2=1.\tag{3}$$

For the force interaction of the phases, we have

$$f_1=\frac{3}{8}\frac{m_2\rho_{11}}{r_p}C_D(u_1-u_2)|u_1-u_2|,\tag{4}$$

where C_D is the drag coefficient of a spherical particle and r_p is the particle radius. In the Stokes flow regime, the drag coefficient is $C_D=24/\mathrm{Re}$, where $\mathrm{Re}=2r_p|u_1-u_2|\rho_{11}/\mu$ is the relative Reynolds number and μ is the viscosity of the gas. Expression (4) in the Stokes flow regime is given by

$$f_1=\frac{(u_1-u_2)\rho_2}{\tau_{st}},\quad \tau_{st}=\frac{2}{9}\frac{\rho_{22}r_p^2}{\mu},$$

where τ_{st} is the Stokes relaxation time of the velocities.

2. SHOCK WAVE STRUCTURE

On the basis of the mathematical model of a mixture with two pressures, we consider the problem of determining the structure of a running shock wave (SW) with the gas pressure gradient taken into account in the momentum conservation equation for the particle phase and with the volume particle concentration taken into account in the equation of state of the gas phase. In this case, Eqs. (1) in a coordinate system fixed to the SW front are

$$\rho_1u_1=\rho_{10}u_0\equiv C_1,\quad \rho_2u_2=\rho_{20}u_0\equiv C_2,\tag{5}$$

$$C_1\dot u_1+m_1\dot p_1=f_1,\quad C_2\dot u_2+m_2\dot p_1+\dot p_2=-f_1.\tag{6}$$

The symbol 0 denotes an initial equilibrium state of the mixture, i.e., the constants C_i are determined by the initial state. Solving system (5), (6) for the derivatives, we bring it to the normal form

$$\frac{du_1}{dx}=\frac{\Delta_{u_1}}{\Delta},\quad \frac{du_2}{dx}=\frac{\Delta_{u_2}}{\Delta},\tag{7}$$

where

$$\begin{gathered}\Delta = \rho_1\rho_2 u_1^2 u_2^2 - m_1 p_{1,\rho_1}\rho_1\rho_2 u_2^2 - \left(m_2 p_{1,\rho_2} + p_{2,\rho_2}\right)\rho_1\rho_2 u_1^2 \\ + m_1 p_{1,\rho_1}\left(m_2 p_{1,\rho_2} + p_{2,\rho_2}\right)\rho_1\rho_2 - m_1 m_2 p_{1,\rho_2} p_{1,\rho_1}\rho_1\rho_2, \\ \Delta_{u_1} = -f_1 u_1\rho_2\left(-u_2^2 + p_{1,\rho_2} + p_{2,\rho_2}\right), \quad \Delta_{u_{2,x}} = f_1\rho_1 u_2\left(-u_1^2 + p_{1,\rho_1}\right), \\ \rho_1 = \frac{C_1}{u_1}, \quad \rho_2 = \frac{C_2}{u_2}, \quad m_2 = \frac{C_2}{\rho_{22}u_2}, \quad m_1 = 1 - m_2, \\ C_1 = m_{10}\rho_{11}u_0, \quad C_2 = m_{20}\rho_{22}u_0, \quad m_{10} + m_{20} = 1, \\ p_{1,\rho_1} = \frac{a_1^2}{1 - \rho_2/\rho_{22}}, \quad p_{1,\rho_2} = \frac{a_1^2\rho_1}{\rho_{22}\left(1 - \rho_2/\rho_{22}\right)^2}, \quad p_{2,\rho_2} = a_2^2.\end{gathered} \tag{8}$$

Consider the motion of the mixture in the phase plane of the phase velocities. Summing up conservation equations (6), we obtain the following momentum conservation law for the mixture as a whole:

$$\Phi_1(u_1,u_2) = \frac{C_1}{u_1}\left(u_1^2 - \left(u_0 + \frac{a_1^2}{u_0(1-m_{20})}\right)u_1 + \frac{a_1^2}{1 - \dfrac{C_2}{\rho_{22}u_2}}\right) + \frac{C_2}{u_2}\left(u_2^2 - \left(u_0 + \frac{a_2^2}{u_0}\right)u_2 + a_2^2\right) = 0. \tag{9}$$

This dependence represents a closed curve in the (u_1,u_2) plane. Note that the form of the gas equation of state imposes a constraint on the proposed model, namely, the initial particle concentration m_{20} and the current velocity u_2 have to satisfy the inequality

$$m_{20} < \frac{u_2}{u_0} = m_u < 1,$$

i.e., the linear representation of the partial equation of state imposes a similar constraint on the domain of admissible volume particle concentrations and, naturally, on the gas concentrations.

2.1. Heuristic Derivation of the Shock Wave Condition for the Discrete Phase in the Gas–Particle Mixture

The equation of motion of the particles in a dense gas mixture can be rewritten as

$$C_2 u_2' + m_2 p_1' + \frac{m_2 p_2'}{m_2} = f_2. \tag{10}$$

Define the function $P_2 = \int \dfrac{dp_2}{m_2}$. Then (10) can be written as

$$r m_2\left(\frac{u_2^2}{2} + \frac{p_1}{r} + \frac{P_2}{r}\right)' = f_2. \tag{11}$$

Let $I_2 = \dfrac{u_2^2}{2} + \dfrac{p_1}{r} + \dfrac{P_2}{r}$. Equation (11) is integrated by parts over the discontinuity located in the interval $(-\varepsilon, \varepsilon)$. According to [16], we take the limit of this expression as $\varepsilon \to 0$ to obtain

$$[m_2 I_2] - [m_2] I_2(0) = \lim_{\varepsilon\to 0} f_2 = 0. \tag{12}$$

Here, $I_2(0) = \lim_{\varepsilon\to 0}\int_{-\varepsilon}^{+\varepsilon} I_2[m_2]\delta(\xi)d\xi$ corresponds to the momentum flow across the strong discontinuity and can be specified. For this purpose, we use the representation

$$[m_2 I_2] = m_2[I_2] + I_{20}[m_2].$$

Substituting it into (12) and setting $I_2(0) = I_{20}$, we find that

$$[I_2] = 0,$$

provided that the volume particle concentration does not vanish anywhere.

Note that a similar approach to the determination of $I_2(0)$ at a physical level of rigor was used in the publications of V.G. Dulov, I.K. Yaushev, A.N. Kraiko, P.G. LeFloach, Mai Duc Thanh, et al.

2.2. Frozen SW

It can be seen that the second nonconservative equation in (6) admits an integral describing a momentum conservation condition for the particle phase. In the case of linear equilibrium mixture equations, we obtain

$$\frac{u_2^2 - u_{20}^2}{2} + \frac{p_1 - p_{10}}{\rho_{22}} + a_2^2 \ln\frac{\rho_2}{\rho_{20}} = 0,$$

whence, in view of (2) and (5), the momentum conservation condition for the particle phase is finally written as

$$\Phi_2(u_1, u_2) = \frac{u_2^2 - u_0^2}{2} + \frac{a_1^2 C_1}{\rho_{22}} \frac{1/u_1}{1 - \dfrac{C_2}{u_2\rho_{22}}} - \frac{a_1^2 C_1}{\rho_{22}} \frac{1/u_0}{1 - \dfrac{C_2}{u_0\rho_{22}}} + a_2^2 \ln\frac{u_0}{u_2} = 0. \tag{13}$$

The intersection points $(\overline{u}_1, \overline{u}_2)$ of the curves $\Phi_1(u_1, u_2) = 0$ and $\Phi_2(u_1, u_2) = 0$ (if they exist) determine the flow parameters behind the front of the frozen SW.

2.3. Equilibrium SW

The equilibrium parameter values in the mixture behind the SW front can be found as follows. Setting $u_1 = u_2 = u$ in (6), after some transformations, we obtain a polynomial of third degree for determining these parameters in the equilibrium SW:

$$u^3 - (\alpha C_{12} + C_3/C_{12})u^2 + \left(a_1^2\xi_1 + a_2^2\xi_2 + \alpha C_3\right)u - \alpha a_2^2 \xi_2 C_{12} = 0, \tag{14}$$

where $C_{12} = C_1 + C_2$, $C_3 = C_{12}u_0 + p_{10} + p_{20}$, $\xi_i = C_i/C_{12}$, $\alpha = \xi_2/\rho_{22}$, and $i = 1, 2$. Obviously, $u = u_0$ is a root of Eq. (14), while one of the other two roots is the terminal equilibrium state $u = u_k$. Note that the root of (14) that does not lie on curve (9), which describes the momentum conservation law for the mixture, is naturally dropped.

Thus, we have determined the parameters behind frozen and equilibrium SWs. Now, solutions can be constructed using the mathematical model of the SW structure in a nonequilibrium mixture of a gas and solid particles, assuming that the gas pressure depends on the mean density of the gas and the incompressible particles. In this way, the results of [12, 13] can be extended to the general case of the adjoint MHM formulation (when the gas pressure is a function of the mean phase densities).

3. RESULTS

3.1. Test: Frozen SWs (One- and Two-Front Configurations)

For $u_0 > a_2 > a_1$ ($u_0 = 460$, $a_2 = 450$, $a_1 = 390$ m/s) in the range of concentrations $m_{20} \in (2\times10^{-4}, 2\times10^{-2})$, the numerical results produced by the present model with $p_1 = p_1(\rho_1, \rho_2)$, $p_2 = p_2(\rho_2)$ agree with the SW structure computed using the model of [13], where the gas pressure is independent of the particle concentration, i.e., $p_1 = p_1(\rho_1)$. The functions $\Phi_1(u_1, u_2) = 0$ and $\Phi_2(u_1, u_2) = 0$ determined by relations (9) and (13) and the Rayleigh–Michelson line through the points u_0 and u_k are shown in Fig. 1 (for $m_{20} = 2\times10^{-4}$). Here, the closed curve $\Phi_1(u_1, u_2) = 0$ is represented by the momentum conservation equation (9) for the mixture. The points 0 and K are the initial and terminal states of the mixture. Moving along this curve from the initial to terminal point, we meet a point of solution blowup at which the gradients of the flow parameters grow to infinity. This situation can be overcome by passing to the lower part of the function $\Phi_1(u_1, u_2) = 0$ with the help of the conditions on the frozen SW. As a result, the curve transfers in a jump to the point f, at which the velocity of the second phase is u_{2f}. Next, we move along the lower part of this curve until the velocity in the second phase reaches the terminal velocity. In the first phase at the given point, the transition to the terminal equilibrium state occurs by means of the frozen SW in the

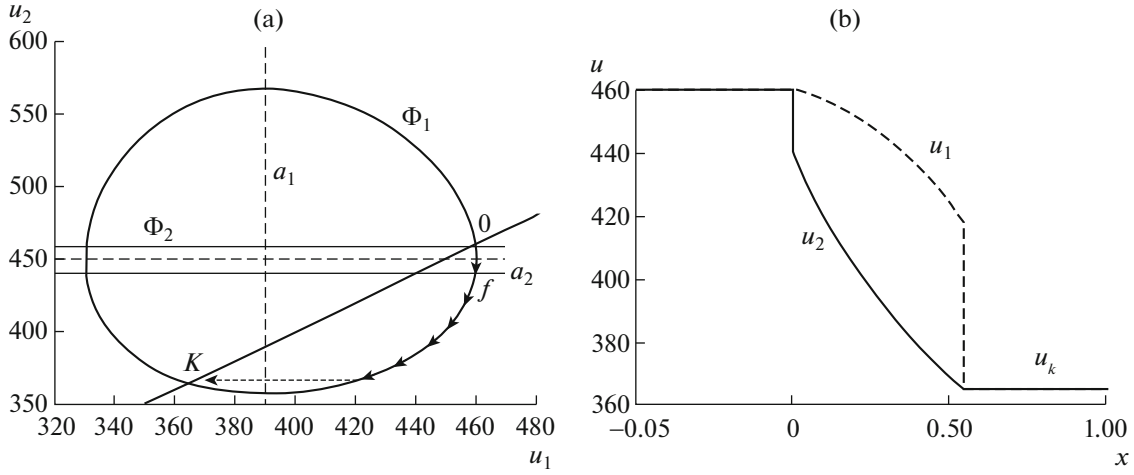

Fig. 1. Frozen two-front SW: (a) phase diagram and (b) phase velocities.

first phase. Thus, we have constructed an SW with a two-front configuration having a head and a tail strong discontinuity. The terminal equilibrium velocities $u_1 = u_2 = u_k$ for the model of [13] and the present model are given in Table 1. It can be seen that their values are similar for the particle concentrations under consideration.

Note that the concept of a two-front SW was used in analyzing the structure of strong discontinuities in the case of the Baer–Nunziato model in [14, 15] and also in [12, 13], where this type of SW was described in detail for two versions of the Anderson model. At high particle concentrations, the transition from the initial state of the mixture to its terminal state with $u_1 = u_2 = u_k$ occurs by means of a shock wave in the gas. As the particle concentration increases, the function Φ_1 deforms, namely, flattens in u_2 and stretches in u_1, while the function Φ_2 changes insignificantly. In this case, a one-front SW appears as the particle concentration is increased.

3.2. Types of SW for $a_2 < u_0 < a_1$ and $u_0 > a_1$

The shock wave structures arising in this case can be analyzed as follows. First, the terminal phase velocity is computed as a function of the mixture state parameters. Then the momentum conservation equations for the mixture, the condition on the strong discontinuity in the second phase, etc., are analyzed in the phase plane of (u_1, u_2). The corresponding numerical results are presented in the subsequent sections.

Terminal equilibrium velocity in SW. Figure 2 shows the terminal equilibrium SW velocity u_k as a function of the initial particle concentration m_{20} and the initial mixture velocity. In contrast to [13], the speed of sound in the first and second phases was set to $a_1 = 330$ m/s and $a_2 = 50$ m/s, respectively. This agrees with the physical view of sound propagation in a granular medium. The initial equilibrium mixture velocity u_0 varied from 100 to 300 m/s, i.e., $a_2 < u_0 < a_1$. The solid curves show the terminal equilibrium SW velocity as a function of the initial particle concentration $u_k = u_k(m_{20})$, while the dashed lines depict $u = u_0$. It can be seen that the terminal velocity u_k decreases with growing u_0; moreover, $u_k > u_0$ if the ini-

Table 1. Phase velocities in the terminal equilibrium shock wave for $u_0 = 460$ m/s

m_{20}	u_k, m/s	
	$p_1 = p_1(\rho_1)$	$p_1 = p_1(\rho_1, \rho_2)$
2×10^{-4}	364.7	364.8
2×10^{-3}	420.4	420.6
2×10^{-2}	437.9	438.1

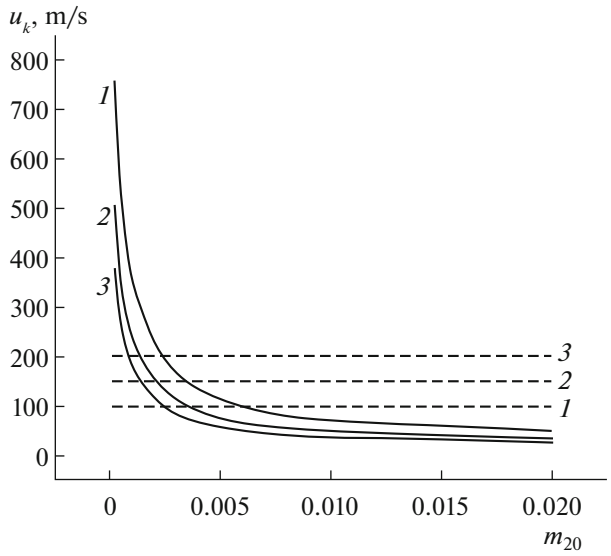

Fig. 2. Terminal equilibrium velocity as a function of the initial particle concentration: $u_k = u_k(u_0)$ (solid) and $u = u_0$ (dashed) for $u_0 =$ (*1*) 100, (*2*) 200, and (*3*) 300 m/s.

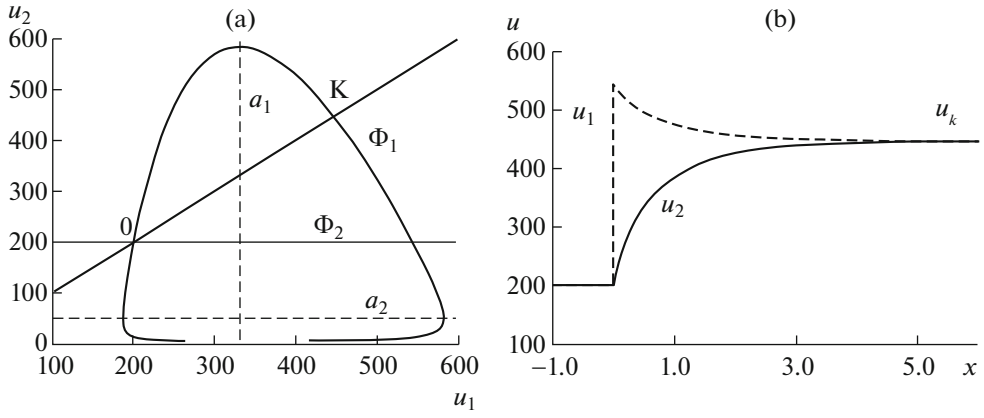

Fig. 3. Dispersive-frozen rarefaction SW: (a) phase diagram and (b) velocity distributions of the phases.

tial particle concentrations are lower than a critical value and $u_k < u_0$ in the opposite case. For $m_{20} > 0.02$, the values of u_k vary weakly in all cases and can slightly increase. Obviously, in areas of initial mixture states where the initial flow velocity is lower than the terminal one, stationary solutions are represented by a rarefaction shock wave. Of course, they are unstable, i.e., they do not exist as solutions of the Cauchy problem within the framework of unsteady flow. Nevertheless, for the subsequent nonstationary analysis of solutions having a nonmonotone distribution of parameters over the wavefront, this type of SW will be briefly described below.

Dispersive-frozen rarefaction SW. Consider the case of dispersive-frozen rarefaction waves. As before, let $a_2 = 50$, $u_0 = 200$, and $a_1 = 330$ m/s and $m_{20} = 10^{-4}$. Figure 3 shows the functions $\Phi_1(u_1, u_2) = 0$ and $\Phi_2(u_1, u_2) = 0$ determined by relations (9) and (13) and the line $u_1 = u_2$ through the points u_0 and u_k.

Using, as initial data for system (7), the mixture parameters $u_{1f} = 544.5$ and $u_{2f} = 200$ on the frozen SW (i.e., the intersection point of $\Phi_1(u_1, u_2) = 0$ and $\Phi_2(u_1, u_2) = 0$ is other than u_0) and solving the boundary value problem for the system of ordinary differential equations, we obtain a solution in the form of an unstable dispersive-frozen rarefaction SW, as shown in Fig. 3, which transfers the mixture to the ter-

Table 2. Terminal equilibrium velocities and types of SW depending on m_{20} and $a_2 = 50$ for $a_1 = 330$ m/s

m_{20}	$u_0 = 100$	$u_0 = 200$	$u_0 = 460$
10^{-4}	892.9 (RSW)	446.8 (RSW)	194.3 (FDSW)
10^{-3}	351.5 (RSW)	176.4 (DSW)	77.1 (FDSW)
10^{-2}	70.8 (DSW)	36.5 (DFSW)	18.6 (2FSW)
10^{-1}	31.9 (DFSW)	24.8 (DFSW)	47.2 (2FSW)

minal equilibrium state $u_k = 446.8$ m/s. In this wave, the gas velocity increases at the jump, which suggests that the gas is in a rarefaction state. Subsequently, behind the front of the frozen rarefaction SW, the gas velocity in the first phase decreases to the terminal value due to friction, whereas the particle velocity increases from the initial value to the terminal equilibrium. Naturally, the pressures behave in an inverse manner.

For the subsequent numerical analysis of SW types, Table 2 presents the terminal equilibrium velocities and the type of flow occurring for various initial states of the mixture in the case of a rarefaction shock wave (RSW), dispersive-frozen shock wave (DFSW), dispersive shock wave (DSW), and two-front shock wave (2FSW). When the initial mixture velocities lie in the dispersion interval (a_2, a_1), it can be seen that, for low particle concentrations up to some limiting value $m_{20} = m_*$, the SW structure problem has no stable solution, i.e., only rarefaction SWs are determined. Then, for $m_{20} > m_*$, the solution exists in the form of a dispersive SW as long as the terminal velocity of the mixture is higher than the speed of sound in the second phase. This regime is observed as long as $m_{**} > m_{20} > m_*$, i.e., there appears another critical volume particle concentration m_{**} determining the type of SW. As the particle concentration increases further, i.e., for $m_2 > m_{**}$, a frozen-dispersive SW is formed in the mixture. In this wave, the terminal mixture velocity is lower than the speed of sound in the second phase, so it ends with a tail jump in the second phase. Finally, for $m_{20} > m_u$, the solution ceases to exist, since the model becomes inapplicable. Let us describe these types of SW.

Fully dispersive SW. Consider the case $a_2 = 50$, $u_0 = 100$, $a_1 = 330$, $u_k = 70.76$ m/s, and $m_{20} = 10^{-2}$. Figure 4 shows the determining conservation laws and the plots of the phase velocities. In this case, it is possible to continuously pass from the initial state (u_0, u_0) to the terminal one (u_k, u_k). In the numerical solution, the computation started from a perturbed point of the initial state. Namely, we set $\overline{u}_1 = u_0 - \varepsilon$,

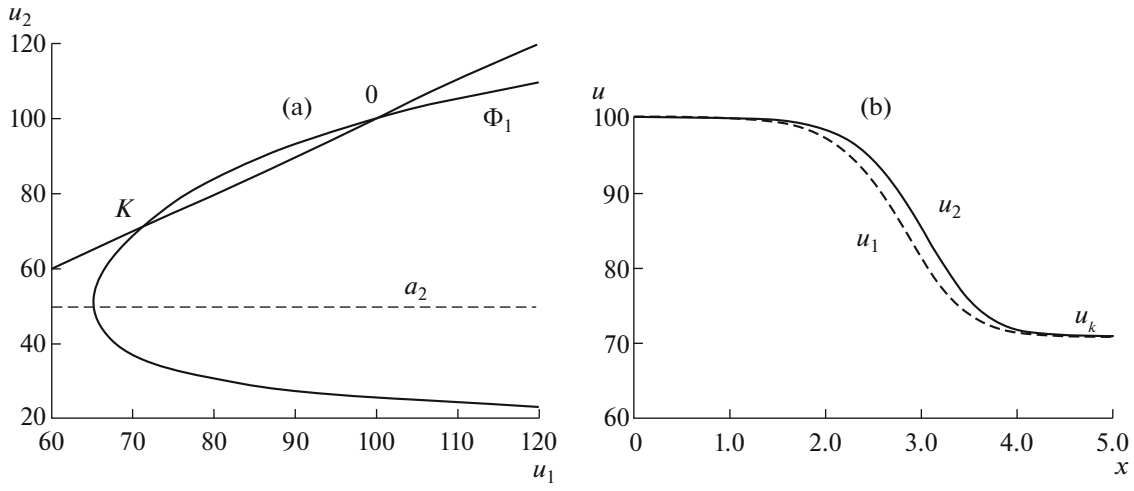

Fig. 4. Dispersive SW: (a) phase diagram and (b) phase velocities for $m_{20} = 10^{-2}$, $u_0 = 100$, and $u_k = 70.76$ m/s.

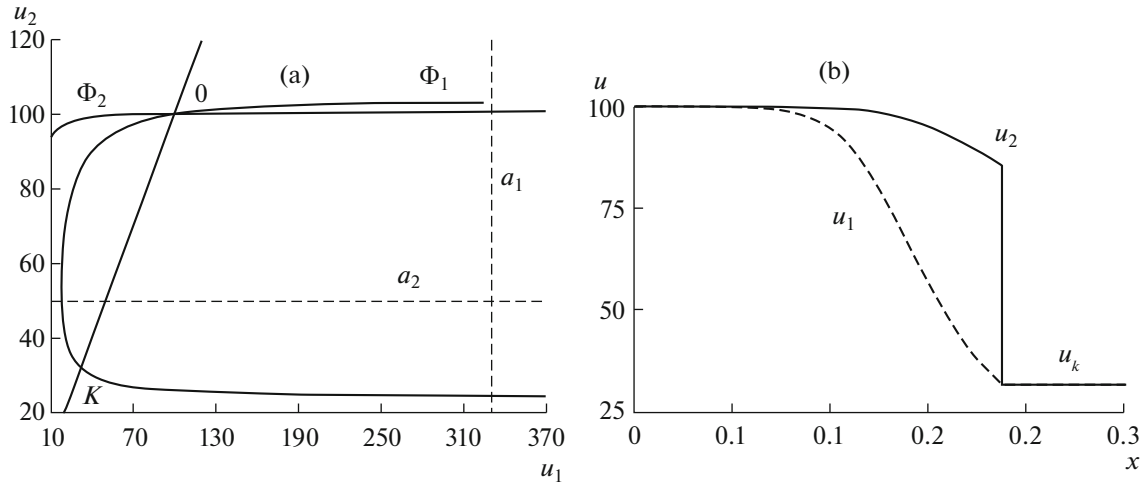

Fig. 5. Dispersive-frozen SW for $m_{20} = 10^{-1}$, $u_0 = 100$, and $u_k = 36.49$ m/s.

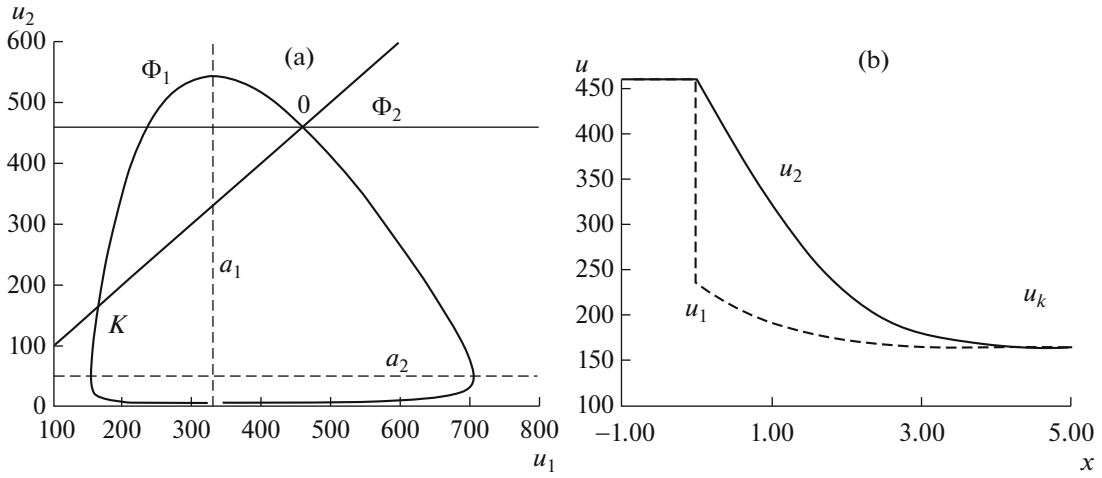

Fig. 6. Frozen-dispersive SW for $m_{20} = 2 \times 10^{-4}$, $u_0 = 460$, and $u_k = 165.1$: (a) phase diagram and (b) phase velocities.

while $\overline{u}_2$ was found using the relation $\Phi_1(u_0 - \varepsilon, \overline{u}_2) = 0$. As a result, the boundary conditions thus chosen for solving the boundary value problem satisfied the momentum conservation law for the entire mixture. The terminal state was reached due to its stability. The resulting SW structure is displayed in Fig. 4. It can be seen that the particles initially move more rapidly than the gas. Then they slow down, their velocity becomes equal to the gas velocity, and the mixture passes to the terminal equilibrium state. The existence of fully frozen and dispersive-frozen shock waves for $u_0 > a_1$ can be shown in a similar manner [12, 13].

Dispersive-frozen SW. Let $a_2 = 50$, $u_0 = 100$, $a_1 = 330$ m/s, and $m_{20} = 10^{-1}$. In this case, the parameters of the mixture in the SW head vary continuously. When the mixture slows down, a sonic singularity in the second phase can arise in the flow. Therefore, we need to introduce a tail SW for passing to the terminal equilibrium state (Fig. 5).

Frozen-dispersive SW. In a similar fashion, we can obtain frozen-dispersive SWs, which exist for $u_0 > a_1$. Figure 6 shows (a) the phase diagram of the conservation laws and (b) the velocities of the phases for mixture parameters $m_{20} = 2 \times 10^{-4}$, $a_2 < a_1 < u_0 = 460$, $a_1 = 330$, and $a_2 = 50$ m/s. From the initial to terminal points, the mixture passes through a frozen SW in the gas phase with the following phase

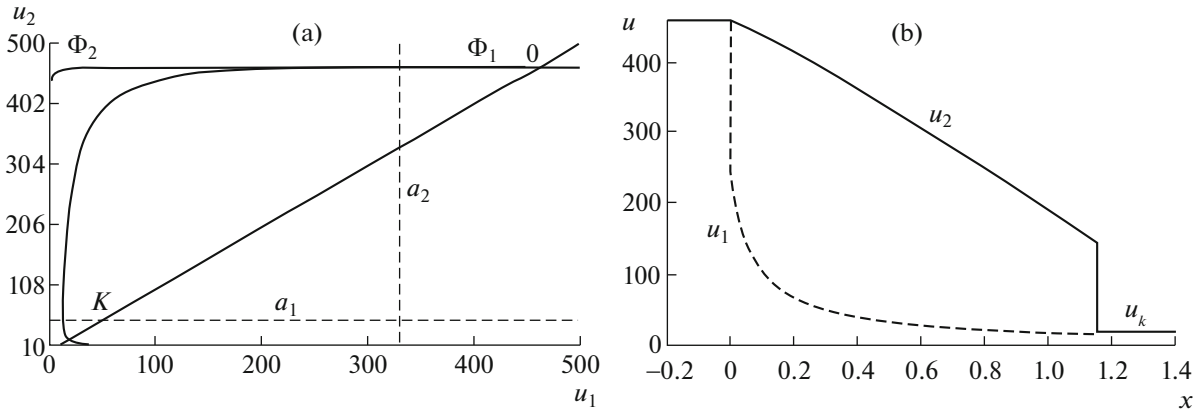

Fig. 7. Two-front SW for $m_{20} = 10^{-2}$, $u_0 = 460$, $u_k = 18.59$ m/s: (a) phase diagram and (b) phase velocities.

velocities behind the strong head discontinuity and in the tail of this structure $\overline{u}_1 = 236.7$, $\overline{u}_2 = 460$, $u_k = 165.1$ m/s.

Two-front SW. As before, the initial velocity of the mixture is higher than the velocity of sound in the gas, while the volume particle concentration is increased: $m_{20} = 10^{-2}$. Presented in Fig. 7, the resulting phase diagram shows that it is possible to pass from the initial to terminal points via a strong discontinuity in the first phase, followed by a zone of velocity relaxation. When the gas velocity reaches its terminal equilibrium value $u_k = 18.6$ m/s, the transition to equilibrium can be performed by means of a tail SW in the particle phase. Figure 7b shows the behavior of the solution for $m_{20} = 10^{-2}$ in the plane of physical variables. We discuss only the mathematical aspects of the problem, without giving a physical interpretation of the resulting types of shock waves. Now let us analyze the stability of these types of shock waves.

4. VERIFYING THE STABILITY OF SOLUTIONS OF CERTAIN TYPES

4.1. Numerical Method

The stability of the resulting stationary solutions of Eqs. (1) was analyzed by applying the mathematical technique for solving problems in the mechanics of heterogeneous media with two pressures and velocities used in [13] for a simpler mathematical model with the mean particle density neglected from the equation of state of the gas.

Time stepping for system (1) was based on a fifth-order scheme of the Runge–Kutta type [17]. The scheme of mth-order accuracy can be described as follows. Let y be one of the unknown functions ρ_i or $(\rho u)_i$ and $Q_y(t)$ be the corresponding components of the vector $\mathbf{Q}$ in Eqs. (1). With the use of this notation, Eqs. (1) can be represented in the form $\dfrac{dy}{dt} + Q_y(t) = 0$.

Then the m-stage scheme is given by

$$\begin{aligned} y^{(0)} &= y^{(n)}, \\ y^{(1)} &= y^{(0)} - \gamma_m \tau Q_y^{(0)}, \\ y^{(2)} &= y^{(0)} - \gamma_{m-1} \tau Q_y^{(1)}, \\ y^{(m)} &= y^{(0)} - \gamma_1 \tau Q_y^{(m-1)}, \\ y^{(n+1)} &= y^{(m)}. \end{aligned} \tag{15}$$

The values of the parameters $\gamma_1, \gamma_2, \ldots, \gamma_m$ are determined by the conditions of approximation and maximum stability. Since the analysis of these conditions for a system of nonlinear differential equations is associated with considerable difficulties, the values of $\gamma_1, \gamma_2, \ldots, \gamma_m$ are calculated by analyzing the linear

transport equation. For the five-stage scheme, these parameters are $\gamma_1 = 1$, $\gamma_2 = 1/2$, $\gamma_3 = 3/8$, $\gamma_4 = 1/6$, and $\gamma_5 = 1/4$. It has been found that, for problems of the given type, this scheme allows one to considerably increase the stability interval and to perform computations with larger Courant numbers. Moreover, the increase in the stability interval was nonlinear in character. For example, the use of the fifth-order accurate scheme made it possible to increase the Courant number by 40 times in comparison with the first-order scheme.

To construct a spatial approximation of system (1) based on the TVD approach [18], it is necessary to split the flux vector $\mathbf{Q}_i$ for each of the components. Numerous methods are available for this purpose. Define $\tilde{p}_1 = m_1 p_1$ and $\tilde{p}_2 = m_2 p_1 + p_2$. In what follows, the index i in fluxes is omitted. To obtain a stable upwind approximation of the right-hand sides of the difference scheme, the flux vector $\mathbf{Q}$ is divided into positive and negative components: $\mathbf{Q} = \mathbf{Q}^+ + \mathbf{Q}^-$. For this purpose, we use the splitting of the flux vector with respect to physical processes [19]. Accordingly, the flux vector $\mathbf{Q}$ is split into components $\mathbf{Q}^+$ and $\mathbf{Q}^-$ depending on the velocity sign so that the pressure is approximated by a downwind scheme, while the other variables are approximated by an upwind scheme:

$$\begin{aligned} Q_\rho^+ &= \begin{cases} \rho u, & u > 0, \\ 0, & u \le 0, \end{cases} \quad Q_\rho^- = \begin{cases} 0, & u > 0, \\ \rho u, & u \le 0, \end{cases} \\ Q_u^+ &= \begin{cases} \rho u^2, & u > 0, \\ \tilde{p}, & u \le 0, \end{cases} \quad Q_u^- = \begin{cases} \tilde{p}, & u > 0, \\ \rho u^2, & u \le 0. \end{cases} \end{aligned} \tag{16}$$

A higher order approximation is obtained using the formulas

$$\frac{\partial \mathbf{Q}}{\partial x} \approx \frac{\left[\mathbf{Q}^+_{j+1/2} - \mathbf{Q}^+_{j-1/2} + \mathbf{Q}^-_{j+1/2} - \mathbf{Q}^-_{j-1/2}\right]}{\Delta x}, \tag{17}$$

where

$$\begin{aligned} \mathbf{Q}^-_{j+1/2} &= \mathbf{Q}^-_{j+1} - \frac{1}{4}\left[(1-\kappa)\Delta^+\left(\mathbf{Q}^-_{j+1}\right) + (1+\kappa)\Delta^-\left(\mathbf{Q}^-_{j+1}\right)\right], \\ \mathbf{Q}^+_{j+1/2} &= \mathbf{Q}^+_{j+1} + \frac{1}{4}\left[(1-\kappa)\Delta^-\left(\mathbf{Q}^+_{j}\right) + (1+\kappa)\Delta^+\left(\mathbf{Q}^+_{j}\right)\right], \\ \Delta^+(\mathbf{Q}_j) &= (\mathbf{Q}_{j+1} - \mathbf{Q}_j), \quad \Delta^-(\mathbf{Q}_j) = (\mathbf{Q}_j - \mathbf{Q}_{j-1}). \end{aligned} \tag{18}$$

The expressions for $\mathbf{Q}^-_{j-1/2}$ and $\mathbf{Q}^+_{j-1/2}$ are derived by shifting the index by unity.

Formulas (17) and (18) approximate spatial derivatives with the third ($\kappa = 1/3$) or second ($\kappa = -1, 0, 1$) order. The approximations represent fully one-sided differences for $\kappa = -1$, central differences for $\kappa = 0$, and upwind differences for $\kappa = 1/3, 1$.

To preserve the monotonicity of the solution in high-gradient regions, the order of approximation is reduced by applying the minmod limiter to the operators Δ^+ and Δ^- of [18]:

$$\begin{aligned} \delta^+ &= \begin{cases} 0, & \operatorname{sign}\Delta^+ \operatorname{sign}\Delta^- \le 0, \\ \min\left(\left|\Delta^+\right|, \Theta\left|\Delta^-\right|\right), & \operatorname{sign}\Delta^+ \operatorname{sign}\Delta^- \ge 0, \end{cases} \\ \delta^- &= \begin{cases} 0, & \operatorname{sign}\Delta^+ \operatorname{sign}\Delta^- \le 0, \\ \min\left(\left|\Delta^-\right|, \Theta\left|\Delta^+\right|\right), & \operatorname{sign}\Delta^+ \operatorname{sign}\Delta^- \ge 0, \end{cases} \end{aligned} \tag{19}$$

where the range of the parameter Θ is given by

$$1 \le \Theta \le \frac{3-\kappa}{1-\kappa}. \tag{20}$$

After introducing the limiter, formulas (18) become

$$\begin{aligned} Q^-_{j+1/2} &= Q^-_{j+1} - \frac{\sigma}{4}\left[(1-\kappa)\delta^+ + (1+\kappa)\delta^-\right]\left(Q^-_{j+1}\right), \\ Q^+_{j+1/2} &= Q^+_{j} + \frac{\sigma}{4}\left[(1-\kappa)\delta^- + (1+\kappa)\delta^+\right]\left(Q^+_{j}\right). \end{aligned} \tag{21}$$

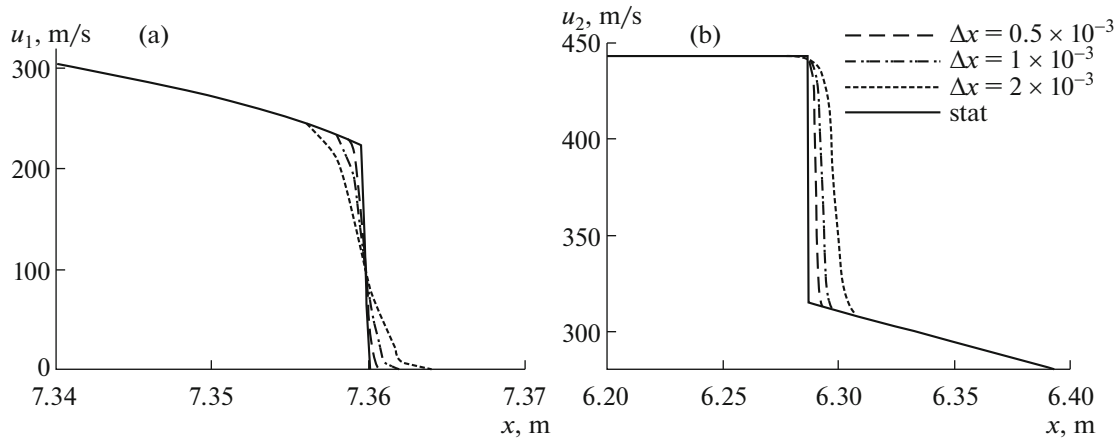

Fig. 8. Grid convergence for a two-front SW.

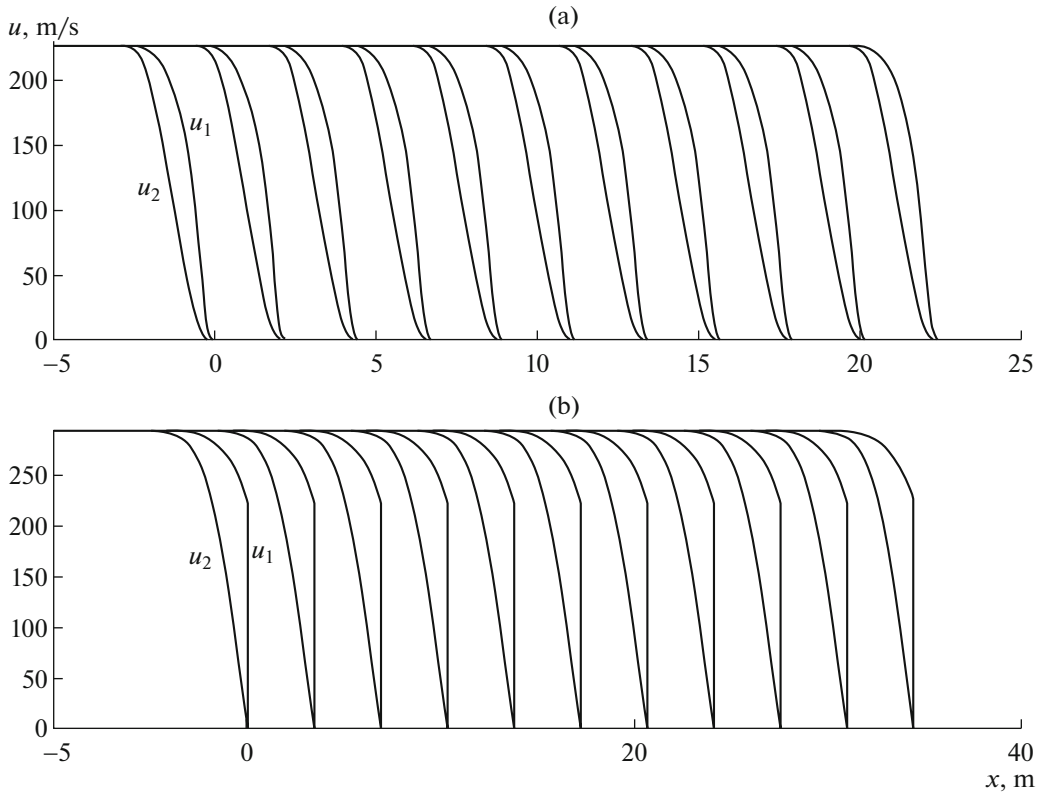

Fig. 9. Shock wave position at various times for two types of SW.

By using the splitting given by formulas (17)–(21), we can construct approximations of the derivatives of the flux components in Eqs. (1); their numerical solution is used to analyze the resolution of several schemes.

The nonconservative terms of Eqs. (1) were approximated using a second-order accurate scheme with central differences

$$\frac{\partial m_i}{\partial x} \approx \frac{m_{i\,j+1} - m_{i\,j-1}}{2\Delta x},$$

where i is the phase index.

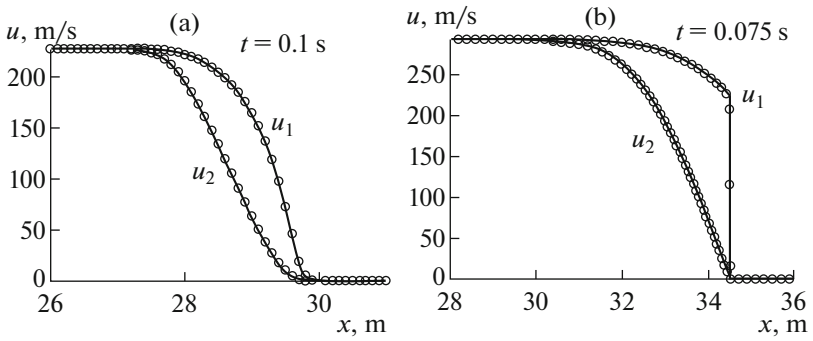

Fig. 10. Comparison of stationary (solid) and nonstationary (circles) solutions for two types of SW.

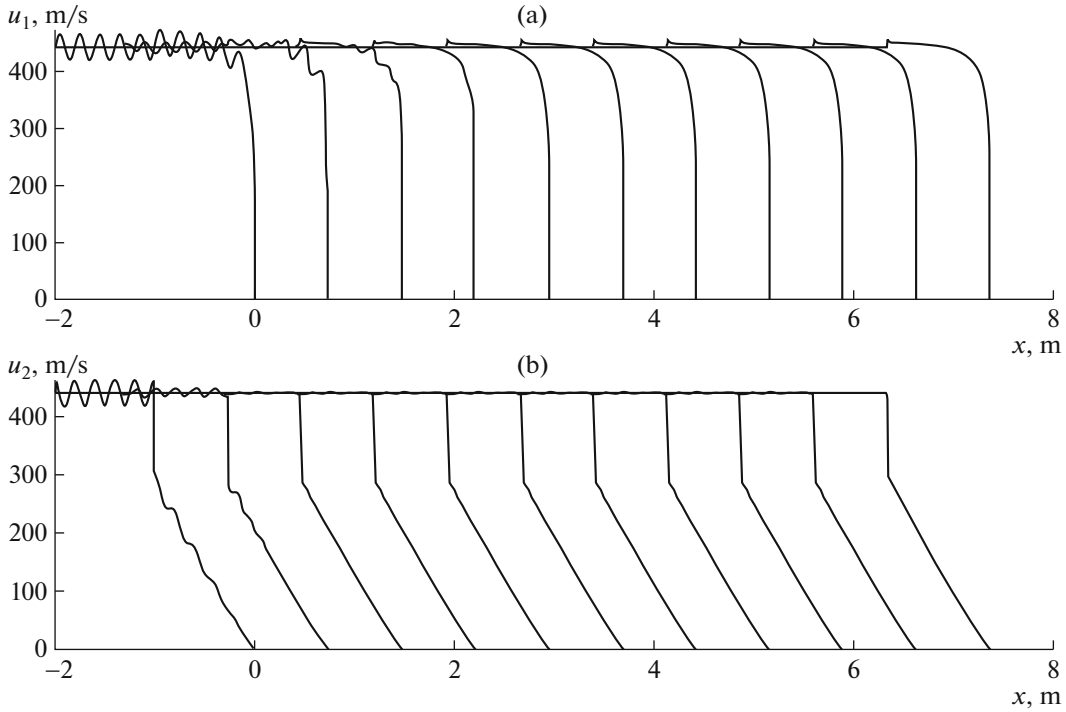

Fig. 11. Stability of a two-front SW with respect to finite perturbations.

4.2. Grid Convergence

The grid convergence of the numerical solution of the two-front SW propagation problem is demonstrated in Fig. 8. For both velocities, the figure shows only a portion of the dispersion interval of the SW, namely, the structure of the frozen SW in the form of a stationary solution (solid curve) and several solutions on refined meshes. It can be seen that, as the mesh size is reduced, the numerical solutions become indistinguishable. The Courant number was set to 0.5. Note that the numerical solution profiles in Fig. 8a intersect at a single point, which was called the center of a finite-difference shock wave in [20]. Such a point is not observed for the tail SW profiles (Fig. 8b), which can possibly be explained by the preceding dispersion interval of this wave structure.

4.3. Stability with Respect to Infinitesimal and Finite Perturbations

Let us discuss the stability of some types of stationary solutions. Figure 9 shows the shock wave position at various times for (a) fully dispersive SWs and (b) SWs frozen in the first phase and dispersive in the second. A stationary solution was specified as initial data. This formulation can be thought of as stability anal-

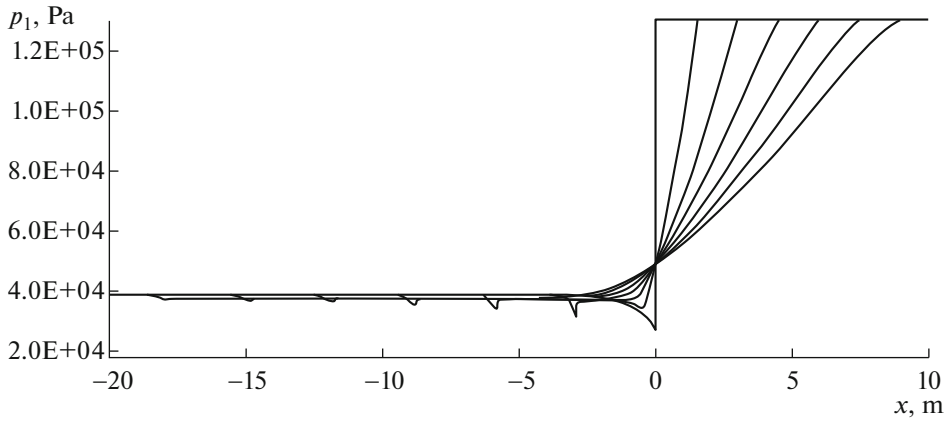

Fig. 12. Propagation of a dispersive-frozen rarefaction SW specified as initial data.

ysis with respect to small (infinitesimal) perturbations, which always arise in the numerical solution. It can be seen that SWs of both types propagate stably in the mixture.

The steady character of propagation is confirmed by Fig. 10, which compares stationary (solid) and nonstationary (circles) solutions for these two types of SW. The stationary solution specified as initial data for the nonstationary problem remains nearly unchanged. It can be seen that three points of the numerical solution fall in the frozen SW (Fig. 10b).

Let us analyze the stability of the solution with respect to finite perturbations. Figure 11 shows the propagation of a two-front SW. The initial stationary solution was perturbed by sinusoidal oscillations with an amplitude of 5% of the velocity behind the shock wave. It can be seen that, at the subsequent times, the perturbations are rapidly damped and the wave propagates steadily.

Finally, we discuss a solution with a dispersive-frozen rarefaction SW. It is well known that such a discontinuity cannot propagate steadily. Figure 12 shows the flow field at various times in the case of initial data specified as the solution shown in Fig. 3. The pressure profiles in the gas phase at various times are presented. The unstable initial flow configuration breaks up into two rarefaction waves. The more intensive wave propagates to the right, while the less intensive wave, to the left. Between them, there appears a low-pressure region.

CONCLUSIONS

A fine structure theory of shock waves was developed using an Anderson-type mathematical model (with the gas equation of state taking into account the particle phase) for describing the flow of a mixture of a gas and solid particles with allowance for their pressures. The types of steady shock waves occurring in the flow were determined on the basis of this theory.

A mathematical technique was developed for computing initial–boundary value problems for nonstationary one-dimensional Anderson-type equations for the mechanics of heterogeneous medium. By applying this technique, it was shown that the resulting frozen and dispersive shock waves of various types are stable with respect to infinitesimal and finite perturbations, and the instability of rarefaction shock waves was demonstrated.

ACKNOWLEDGMENTS

This work was supported by the Russian Science Foundation, project no. 16-19-00010.

REFERENCES

1. A. V. Fedorov, V. M. Fomin, and Yu. A. Gosteev, *Dynamics and Ignition of Gas Mixtures* (Novosibirsk. Gos. Tekh. Univ., Novosibirsk, 2006) [in Russian].
2. A. V. Fedorov, V. M. Fomin, and T. A. Khmel', "Heterogeneous detonation," *Combustion Laws*, Ed. by Yu. V. Polezhaev (Energomash, Moscow, 2006), pp. 276–302 [in Russian].

3. A. V. Fedorov, V. M. Fomin, and T. A. Khmel', *Wave Processes in Gas Suspensions of Metallic Particles* (Parallel', Novosibirsk, 2015) [in Russian].
4. Yu. V. Kazakov, A. V. Fedorov, and V. M. Fomin, "Structure of isothermal shock waves in gas suspensions," in *Problems in the Theory of Porous Media Flows and Mechanics of Oil Production Enhancement* (Moscow, 1987), p. 108 [in Russian].
5. A. A. Gubaidullin, A. I. Ivandaev, and R. I. Nigmatulin, "A modified "coarse particle" method for calculating nonstationary wave processes in multiphase dispersive media," USSR Comput. Math. Math. Phys. **17** (6), 180–192 (1977).
6. A. V. Fedorov and V. M. Fomin, "On the theory of combination discontinuities in gas suspensions," in *Physical Gas Dynamics of Reacting Media* (Novosibirsk, 1990), pp. 128–134 [in Russian].
7. T. A. Khmel and A. V. Fedorov, "Modeling of shock wave and detonation processes in collisional particle suspensions in gas," *Proceedings of the 24th ICDERS, July 28–August 2, 2013* (Taipei, Taiwan, 2013).
8. T. A. Khmel' and A. V. Fedorov, "Molecular-kinetic description of dynamic processes in two-phase collisional media," Fiz. Goren. Vzryva **50** (2), 81–93 (2014).
9. A. V. Fedorov, "Structure of a combination discontinuity in gas suspensions in the presence of random pressure from particles," J. Appl. Mech. Tech. Phys. **33** (5), 648–652 (1992).
10. P. G. LeFloch and M. D. Thanh, "The Riemann problem for fluid flows in a nozzle with discontinuous cross-section", Preprint No. NI03024-NPA (Isaac Newton Institute for Mathematical Sciences, University of Cambridge, UK, 2003).
11. T. B. Anderson and R. Jackson, "A fluid mechanical description of fluidized beds," Ind. Eng. Chem. Fundam. **6** (4), 527–539 (1967).
12. A. V. Fedorov, "Structure of shock waves in heterogeneous medium with two pressures," Fiz. Goren. Vzryva **51** (6), 62–71 (2015).
13. I. A. Bedarev and A. V. Fedorov, "Structure and stability of shock waves in a gas-particle mixture with two pressures," Vychisl. Tekhnol. **20** (2), 3–19 (2015).
14. A. V. Fedorov, "Shock-wave structure in a mixture of two solids (a hydrodynamic approximation)," Model. Mekh. **5(22)** (4), 135–158 (1991).
15. A. V. Fedorov and N. N. Fedorova, "Structure, propagation, and reflection of shock waves in a mixture of solids (the hydrodynamic approximation)," J. Appl. Mech. Tech. Phys. **33** (4), 487–494 (1992).
16. O. A. Oleinik, "Discontinuous solutions of nonlinear differential equations," Usp. Mat. Nauk **12** (3), 3–73 (1957).
17. C.-W. Shu and S. Osher, "Efficient implementation of essentially non-oscillatory shock-capturing schemes," J. Comput. Phys. **77** (2), 439–471 (1988).
18. S. R. Chakravathy and S. Osher, "New class of high accuracy TVD schemes for hyperbolic conservation laws," AAIA Paper, No. 85 (0363) (1983).
19. V. M. Kovenya and N. N. Yanenko, *Splitting Methods in Gas Dynamics Applications* (Nauka, Novosibirsk, 1981) [in Russian].
20. A. V. Fedorov, V. M. Fomin, and N. N. Yanenko, "Differential analyzer of discontinuities in solutions of nonhomogeneous hyperbolic equations," Dokl. Akad. Nauk SSSR **254** (3), 554–559 (1980).

Translated by I. Ruzanova